Periodica Polytechnica
Civil Engineering

61(3), pp. 462–470, 2017
https://doi.org/10.3311/PPci.7999

Experimental Investigation on 3D Flow around a Single T-Shaped Spur Dike in a Bend

Mohammad Vaghefi[1*], Masoud Ghodsian[2], Maryam Akbari[1]

RESEARCH ARTICLE

Received 23 February 2015; Revised 25 January 2016; Accepted 21 April 2016

Abstract

The flow field around a T-shaped spur dike located in a 90° bend is investigated experimentally. The three-dimensional Acoustic Doppler Velocimeter (ADV) was used for measuring the flow field. The comparison of the three dimensional components of velocity was made in different sections of the bend and the differences of the flow pattern along the bend was analyzed. The observations showed the significant effect of the spur dike on the secondary flow patterns. Some horizontal vortices with a counter-clock-wise direction were also observed in the up and down stream of the spur dike near the outer bank of the bend. In addition, the vortices and reverse flows in the up and down stream of the spur dike, the changes of the secondary flow and vorticity are also addressed in this study.

Keywords

flow pattern, T-Shaped spur dike, secondary flow, 90 degree bend, vorticity

[1] Department of Civil Engineering, Persian Gulf University, Shahid Mahini Street, Bushehr, P.O.B. 75169-13817, Iran

[2] Department of Civil and Environmental Engineering, Tarbiat Modares University, Jalal Ale Ahmad Highway, Tehran, P.O.B. 14115-111, Iran

[*] Corresponding author, e-mail: vaghefi@pgu.ac.ir

1 Introduction

The variations in riverbed topography and 3-dimensional nature of the flow in bends lead to a formation of a complicated flow at river bends. Presence of centrifugal force and its interaction with the lateral pressure gradients, bring about a flow which is referred to as secondary flow. In such a flow, surface water is driven towards the outer bank while near bed water moves towards the inner bank. This flow significantly affects the river bend's morphology insofar as high velocity in outer bank causes erosion of riverbed and river bank. Usually, spur dikes are used to stabilize bank of the rivers. However, using spur dikes at bends will result in turbulence of flow around spur dikes and will add a further complication to the flow pattern at the outer bank. This is largely due to interaction between the flow pattern induced by spur dike and secondary flows at bends. The flow field around spur dike is a complex phenomenon, involving separation of flow to develop three-dimensional vortex flow; and the complexity increases with the development of the scour hole.

Giri et al. in 2004, carried out experimental and numerical simulations of flow and turbulence in a bend channel with unsubmerged spur dikes. They measured flow velocity by changing the position of spur dikes, and measured vortex field and turbulence intensity two-dimensionally [1]. Nagata et al. in 2005, simulated three-dimensional flow pattern around a single spur dike with live bed. They analysed average flow and studied its relation with the way scour hole is created and expands [2]. Fazli et al. in 2008, did an experimental study on a 90 degree bend channel to study the parameters affecting scour around short and straight spur dikes. The results of the study on bend channel with single spur dike indicates that in developed bends, as the spur dike is moved away from the beginning of the bend, maximum depth of scour rises, whereas this parameter in a steep bend first decreases and then increases [3]. Ghodsian and Vaghefi in 2009, conducted an experimental study on how changes in Froude Number, and length of wing and web of T-shaped spur dike located in a 75 degree position affect flow pattern in a 90 degree bend. They proved that as the length of the spur dike increases, length of separation

zone and the formed vortex in the zone increases [4]. Zhang et al. in 2009, investigated turbulent flow in the local scour hole around a single non-submerged spur dyke experimentally and numerically. They measured the scour geometry and flow velocities in details with a high-resolution laser displacement meter, electro-magnetic velocimetries and PIV (Particle image velocimetry) [5]. Duan et al. in 2009, investigated average and turbulent flow around a straight spur dike located in an experimental channel with rigid bed. They observed that average flow in both lateral and vertical directions separated, and in the circulation zone behind the spur dike, there is a combination of horizontal and vertical vortexes [6]. Naji et al. in 2010, did experimental and numerical studies of flow pattern in a 90 degree bend and concluded that stream lines in the level close to bed orient to inner wall and in the levels near water surface orient to outer wall. Also, the location of the maximum longitudinal velocity at the beginning of the bend is switched to the section's inner half and then toward the channel's outer wall [7]. Duan et al. in 2011, measured three dimensional flow field around an experimental dike structure using a micro ADV. They studied turbulent bursts around the spur dike for the flat and asymptotic bed surface. Moreover, they analysed time fractions of turbulent burst events including outward interaction, ejection, inward interaction, and sweep in each quadrant at the neighbour of the dike before and after the formation of scour hole [8]. Gu et al. in 2011, performed the laboratory experiments to study the characteristics of the flow and the transport of suspended sediment in an open channel with permeable dikes. They investigated the influence of the aspect ratio (d/l) of the interval between dikes (d) to the length of dikes (l) on these characteristics. They concluded that the development of large-scale horizontal eddies requires some distance in a shear layer for permeable dikes, although they are periodically generated from the first dike in the case of impermeable dikes [9]. Chen et al. in 2012, used the compressive VOF (volume of fluid) method to develop the models for water and suspended sediment in a 90 degree bend flume with non-submerged spur dyke at different angles. They simulated local scouring, deposition and resuspension, and analyzed the processes of adsorption and desorption of pollutants on suspended sediment [10]. Sharma et al. in 2012, studied experimentally the flow past a spur dyke on a rigid bed meandering channel with a trapezoidal cross section. To measuring the velocities, they used an acoustic Doppler velocimeter (ADV). They results showed that length of the downstream separation zone changes according to the location of the spur dyke [11]. Vaghefi et al. in 2009 and 2012, placed the T-shaped spur dike in a 90 degree bend, and carried out several experimental studies on the effects of the Froude Number, The length of the spur dike, the position of the spur dike, the radius of curvature, etc. on flow and scour pattern. They concluded that the location of the maximum scour depth is at the distance of 10 to 20 % of spur dike's length and at its upstream. They also observed that increasing the length of the spur dike, decreasing the length of the wing of the spur dike, increasing Froude Number, and positioning the spur dike towards downstream will result in an increase in the dimensions of the scour hole [12-14]. Karami et al. in 2012, studied scour phenomenon around a series of impermeable and nonsubmerged spur dikes using both experimental and numerical methods. They used laser bed-profiler for measuring scour geometry and SSIIM numerical model to compute the sediment transport around the spur dikes. The results showed that there are two distinct zones with different depth and slope in the scour hole. The deeper hole was formed due to a horseshoe vortex, and the shallow hole was formed due to the secondary vortex [15]. Fang et al. in 2013, studied the turbulent flow past a series of groins in a shallow, open channel by large-eddy simulation (LES). They obtained the time-averaged velocities and turbulence intensities at the water surface using particle image velocimetry (PIV) to validate the LES model. Their model results showed that a rectangular-headed groin generates higher turbulence intensities and larger vortices than a round-headed groin [16]. Ibrahim in 2014, used combined physical and numerical models to investigate the effect of implementing oriented groins on the scour and silting processes in a straight channel. They derived simple formulae to evaluate the scour and silting parameters [17]. Vaghefi et al. in 2015, analyzed flow patterns around a T-shape spur dike and a support structure, which is located upstream of the T-shape spur dike in a 90 degree bend by Flow-3D model. They concluded that by increasing support structure distance from 3L up to 9L, the power of secondary flow around main spur dike decreased by 40–120% [18].

This paper present an experimental study of 3-dimensional flow pattern around a T-shaped spur dike located in a 90^{o} bend. The results of velocity components in the longitudinal, lateral and vertical directions are presented. The vortices and reverse flows in the up and down stream of the spur dike, the changes of the secondary flow and vorticity are also addressed in this study.

2 Experiments

Experiments were carried out at the Hydraulic Laboratory of Tarbiat Modares University, Tehran. The main channel consisted of a 7. 1m long upstream and a 5.2m long downstream straight reaches. A 90° channel bend was located between the two straight reaches. The channel was of rectangular cross section 0.6 m width; 0.7 m height with 2.5m radius of bend to centerline. Fig. 1 shows a schematic view of the channel. The bed and sides of channel was made of glass supported by metal frame. Measurement of discharge was done by a calibrated orifice set in the supply pipe. A sluice gate was located at the end of the main channel to control the flow depth. The spur dike was made of Plexiglas (1 cm thick) T shaped in plan. The length of spur dike and its wing was 9 cm. The spur dike was located at 75 degree cross section of the bend. Since the section is regarded

as a critical case in a 90 degree mild bend without spur dike, and the maximum scour occurs at it, according to Vaghefi et al. (2008) studies [19]. Accordingly, a T-shaped spur dike has been placed at 75 degree position to decrease scour at outer wall of the bend. Experiments were conducted with a constant discharge Q=25 l/s with Froude number equal to 0.34 and depth of flow in beginning of the bend 12 cm (Fr=0.34 and Z=12 cm). The 3D components of velocity were measured using ADV (vecterino model). The side-looking probe was used to measure velocity components near-the-surface and down-looking probe was used for measuring velocity components at other layers of flow.

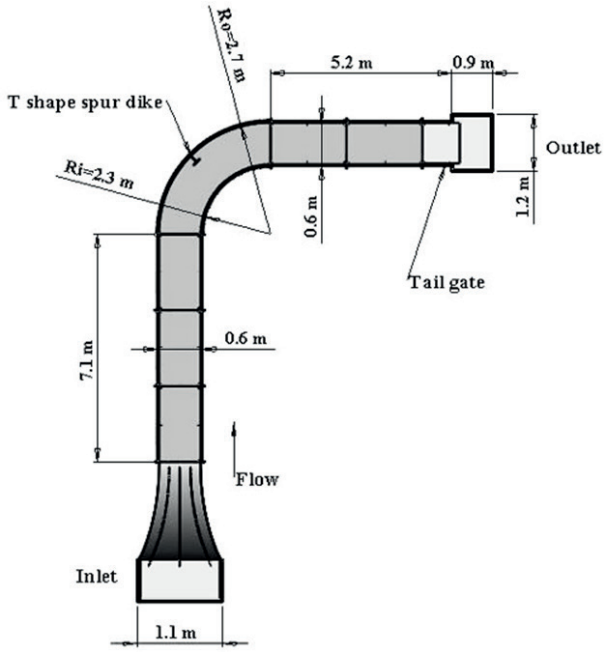

Fig. 1 Schematic view of the channel

The velocimeter was set to 50Hz and measuring time at each grid point was about 60 seconds. For every point and every direction, the device produced 3000 output velocities which were recorded by auxiliary database software, "Vecterino" & "Explore V". To read the flow velocity around wing and web of the spur dike, the probe was set in several directions. The recorded data in were converted from polar coordinates into Cartesian coordinates. In the experiments with the spur dike, velocity profiles were measured at 23 sections along the bend with 5 horizontal levels and 18 points for every lateral axis. For this purpose, non-uniform grid was used which became finer in the vicinity of the spur dike.

3 Result and Discussion

It was found that a secondary flow develops from the beginning of the bend and its strength grows along the bend. A typical lateral component of velocity profiles in two sections at the upstream of the spur dike, are shown in Fig. 2. It was found that at section 30°, a main secondary flow is formed near to the outer bank. While another secondary flows are formed near the inner bank (See Fig. 2(a)). This is due to spur dike's influence on the flow. In the vicinity of spur dike, its influence on flow is more significant. It is evident from Fig. 2(b) that the lateral velocity components in section 72.5° i.e. at a distance of about 1.2 times the length of spur dike toward the upstream, two main counter clockwise secondary flows occurs, one near the bed and the other one near the water surface. However a secondary flow of smaller strength is also formed near the inner bank and close to the water surface.

The lateral component of velocity at the upstream of spur dike and at a distance of 0.65 times spur dike length is shown in Fig. 3(a). It is evident from this figure that two mentioned lateral flows collapse into one lateral flow. At this section a secondary flow, in the zone of spur dike web and inner bank of channel is also formed. The lateral component of velocity at section 74.5°, i.e. near the spur dike web and at a distance of 0.25 times spur dike length is shown in Fig. 3(b). In this section, two secondary flows are observed between the spur dike web and the outer bank. The first one, with a clockwise direction is the main lateral flow. The second lateral flow, with a counterclockwise direction is a result of a low-pressure area near the outer bank. Between wing wall and the inner bank, a clockwise and a counterclockwise secondary flow are observed. Extension of separation area is also noticeable in this section.

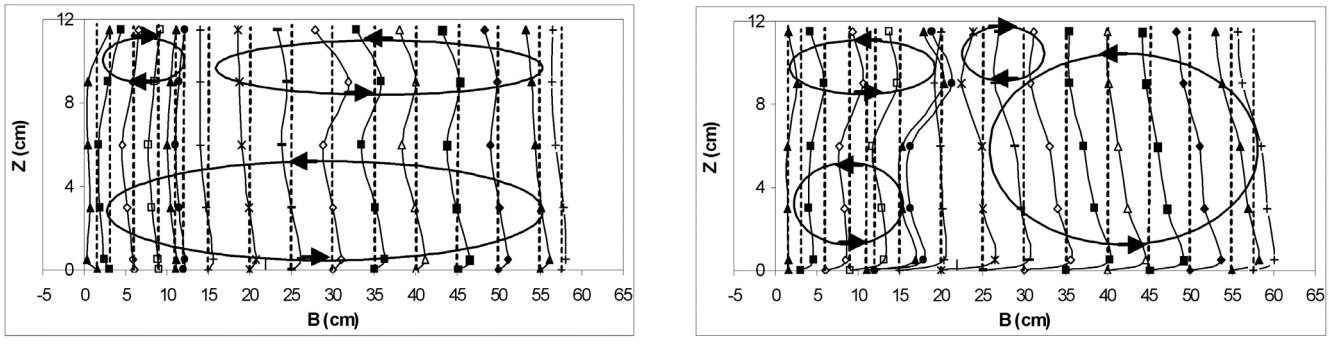

(a) (b)

Fig. 2 Lateral velocity component in the upstream of spur dike at sections: (a) 30° and (b) 72.5°

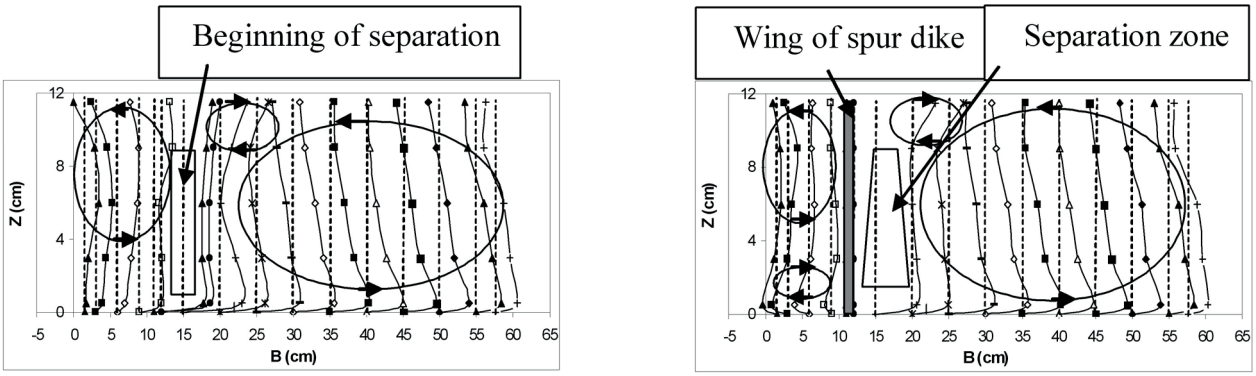

(a) (b)

Fig. 3 Lateral velocity component in the upstream of spur dike at sections: (a) 73.75° and (b) 74.5°

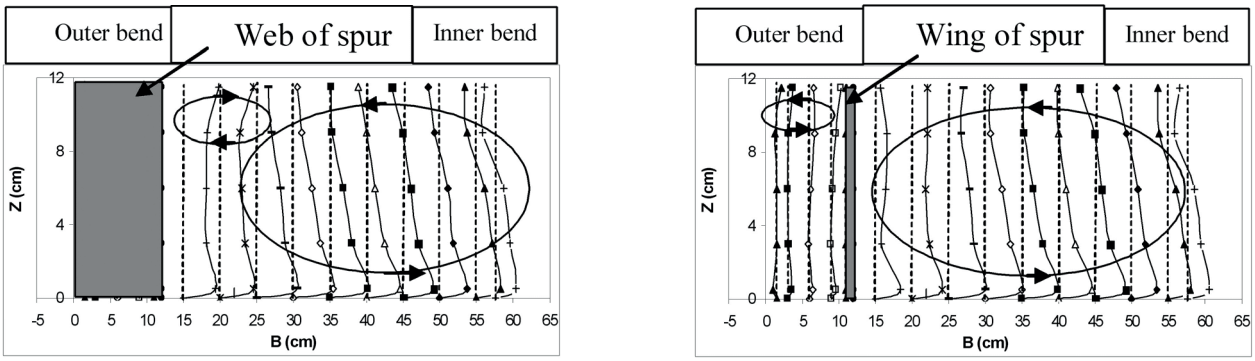

(a) (b)

Fig. 4 Lateral velocity component in the downstream of spur dike at sections: (a) 75° and (b) 75.5°

Fig. 4 shows the lateral component of velocity profiles in the downstream the spur dike. Spur dike web's Front view is shown in Fig. 4(a). A main secondary flow and a second lateral flow near the spur dike wing can be seen in this section. Second lateral flow forms close to the spur dike wing because of the separation area. Fig. 4(b) corresponds to a section near the spur dike web at a distance of 0.25 times the spur dike length. In this section, between the spur dike wing and outer bank, a counterclockwise weak lateral flow forms near the water surface which reflects the existence of upstream inclined flows near the surface. The expansion of flow after the wing causes main secondary flow to be dominant between the wing and the inner bank of channel.

Fig. 5 depicts typical velocity vectors for different lateral sections along the bend. It was found that the effect of spur dike on flow field is noticeable within the upstream distance of about 8 times spur dike length. Existence of rotational flow is observed in all sections. Figs. 5(a) and 5(b) corresponds to upstream and Figs. 5(c) to 5(f) corresponds to downstream of the spur dike. The separation area near the water surface is obvious in Fig. 5(c). The down flow around the spur dike, as is evident in this figure is the cause of scour, in the case of movable bed. The upward flows near the outer bank can be seen in Fig. 5(f). At other sections of the bend, it is observed that the main secondary flow is inclined to the inner bank.

It was found that up to section 60° of the bend, the longitudinal components of velocity profile are not affected by the spur dike. Fig. 6 shows typical longitudinal components of velocity profiles at the upstream of the spur dike. Figs. 6(a) and 6(b) depict sections near the spur dike. It is obvious that longitudinal component of velocity increases at first and second layers near the surface and near the wing of spur dike. This is due to tendency of flow to move towards the low-pressure zone after the spur dike. Fig. 6(b) gives a clearer picture of this phenomenon.

Typical longitudinal components of velocity at and at the downstream of spur dike are shown in Fig. 7. It is evident from Figs. 7a and 7b, which corresponds to section close to the spur dike wing, that longitudinal components of velocity at first and second layers near the wing are higher. By moving towards end of the bend, longitudinal components of velocity at upper and middle layers grow. It should also be noted that near the outer bank, the magnitude of velocity is less. This is due to effect of spur dike and maximum velocity tendency towards channel center which sometimes forms a low-longitudinal-velocity zone and a recirculation flow near the outer bank.

Fig. 8 shows typical vertical components of velocity profiles at sections 73.5° and 74.5° (i.e. at the upstream of spur dike). At a distance of about 1.2 times spur dike length (upstream of the spur dike), downs flows is dominant near the outer bank. This flow has a positive pressure gradient at layers close to the bed.

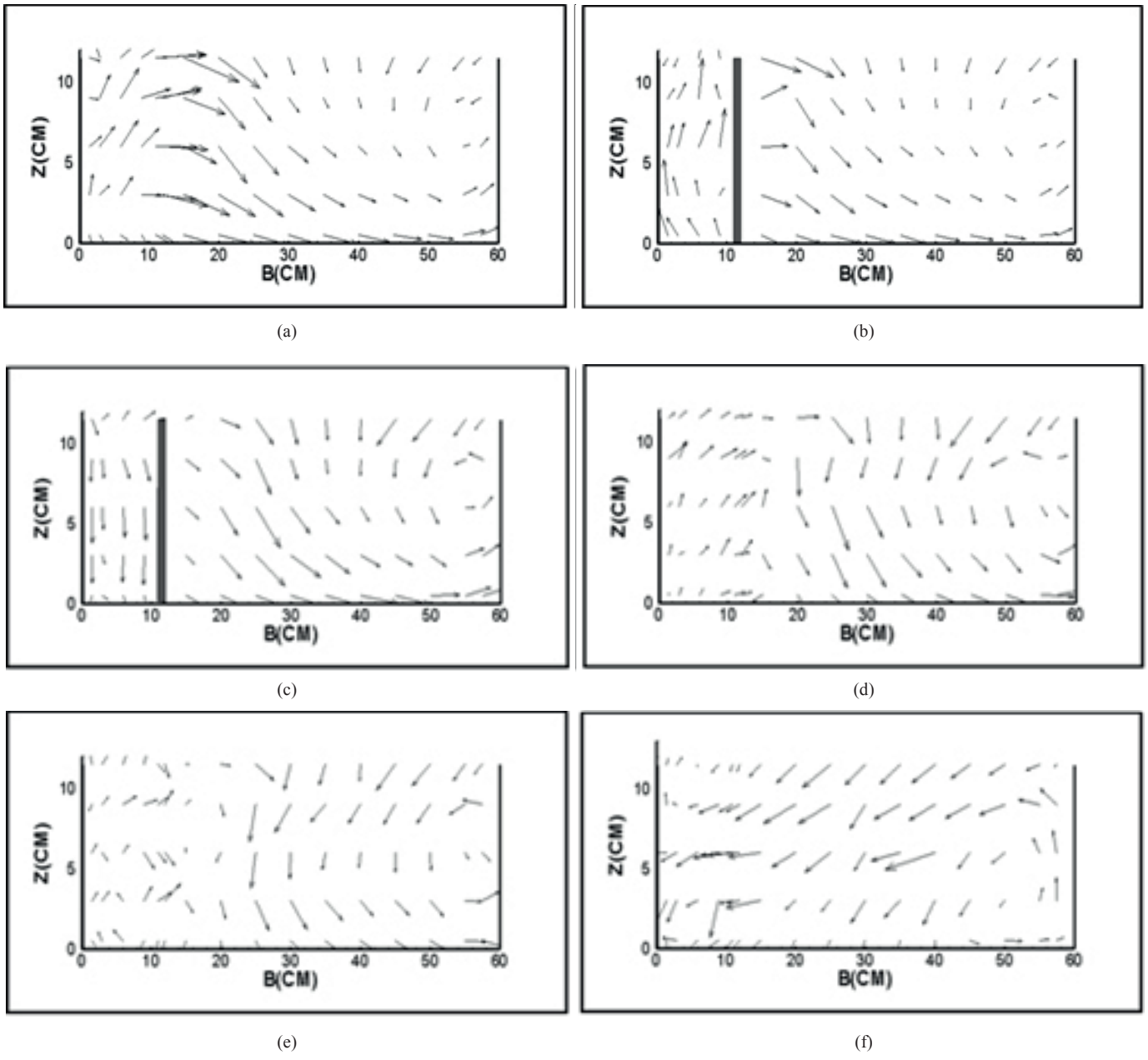

Fig. 5 Velocity vectors at different lateral sections: (a) 73.75 (b) 74.5 (c) 75.5 (d) 77.5 (e) 80 and (f) 90°

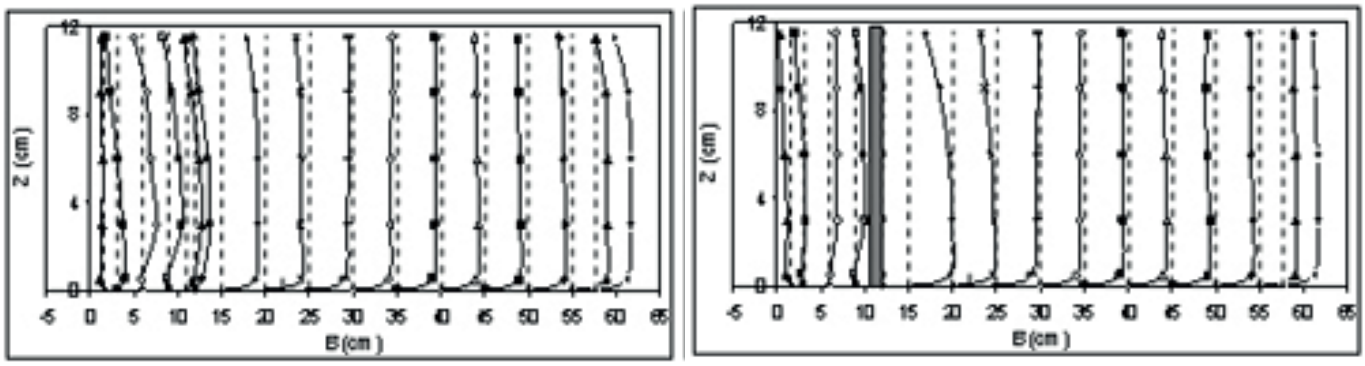

Fig. 6 Longitudinal component of velocity profiles at the upstream of spur dike at sections: (a) 73.75 and (b) 74.5°

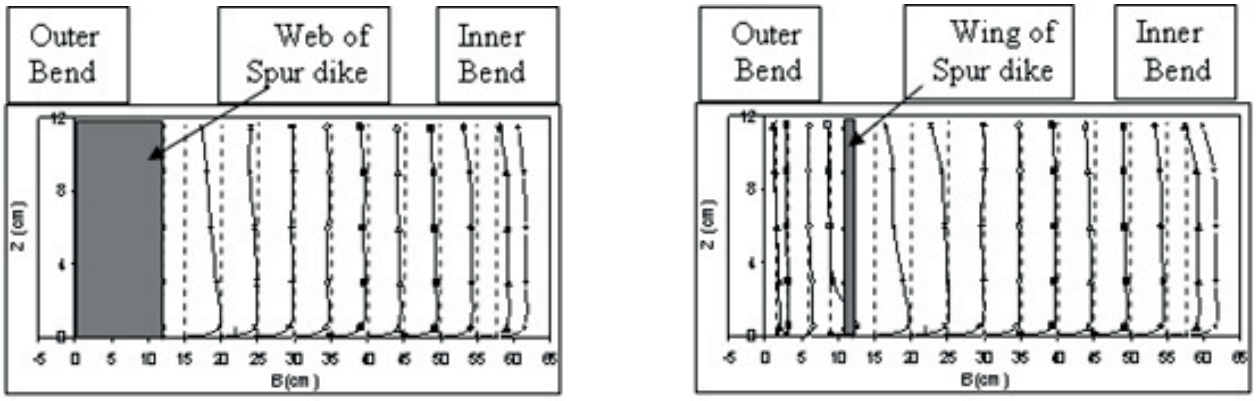

(a) (b)

Fig. 7 Longitudinal component of velocity profiles at downstream of spur dike at sections: (a) 75 and (b) 75.5°

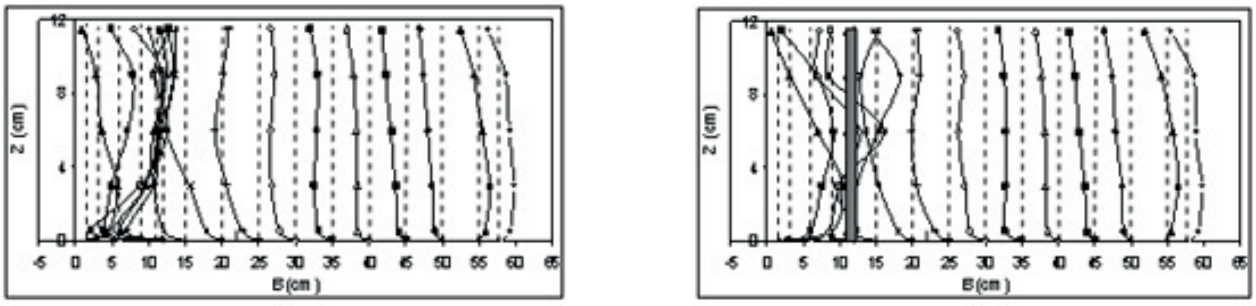

(a) (b)

Fig. 8 Vertical component of velocity profiles at the upstream of spur dike at sections: (a) 73.75 and (b) 74.5°

The inclination of flow toward the bed is also observe. At layers close to the surface, flow is upward because of decrease in flow velocity near the surface. The significant up flow between the spur dike wing and the outer bank is clearly depicted in Figs. 8(a) and 8(b). At middle layers, the strength of this flow is more. The down flow is also noticeable near the inner bank and at upper layers.

Fig. 9 shows typical vertical components of velocity profiles at sections 75° and 75.5°. It is clear that near the bed, a down flow is perceivable for profiles near the spur dike wing. At the inner bank, near the riverbed, an up flow and near the water surface, a down flow is observed. Close section to the spur dike web is shown in Fig. 9(b). Between the wing and the inner bank, the flow pattern remains almost the same for sections 75° and 75.5°. It is evident that from the middle layers to the surface, an up flow is dominant. On the other hand, there is a dominant down flow from the middle layers. The spur dike causes the significant variations in the vertical component of velocity profiles at different layers. But in the vicinity of the inner bank, secondary flows at the bed bring about an up flow at the bed and a down flow at the water surface.

Fig. 10 shows typical velocity vectors at two levels i.e. at distance of 5mm and 115mm from the bed. The velocity vectors, at the downstream of spur dike and near the water surface, is

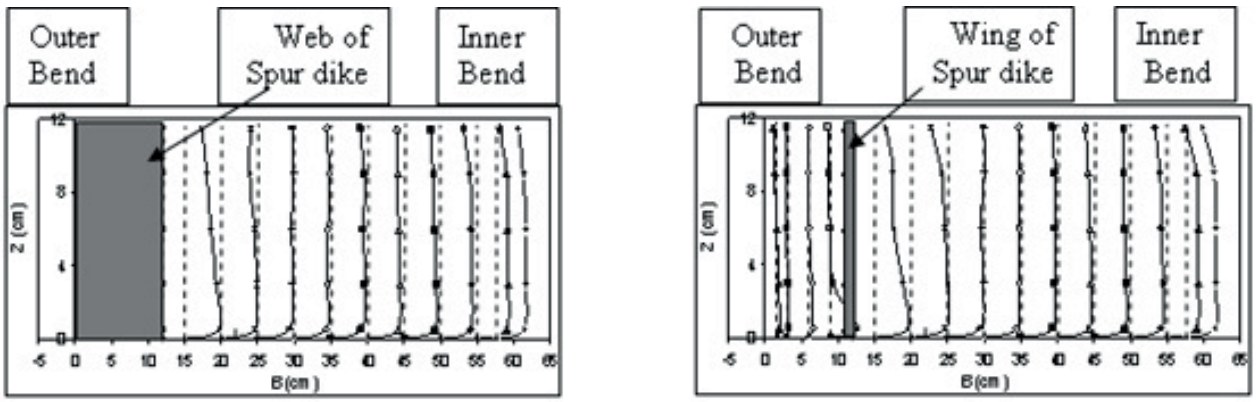

(a) (b)

Fig. 9 Vertical component of velocity at the down stream of spur dike at sections: (a) 75° and (b) 75.5°

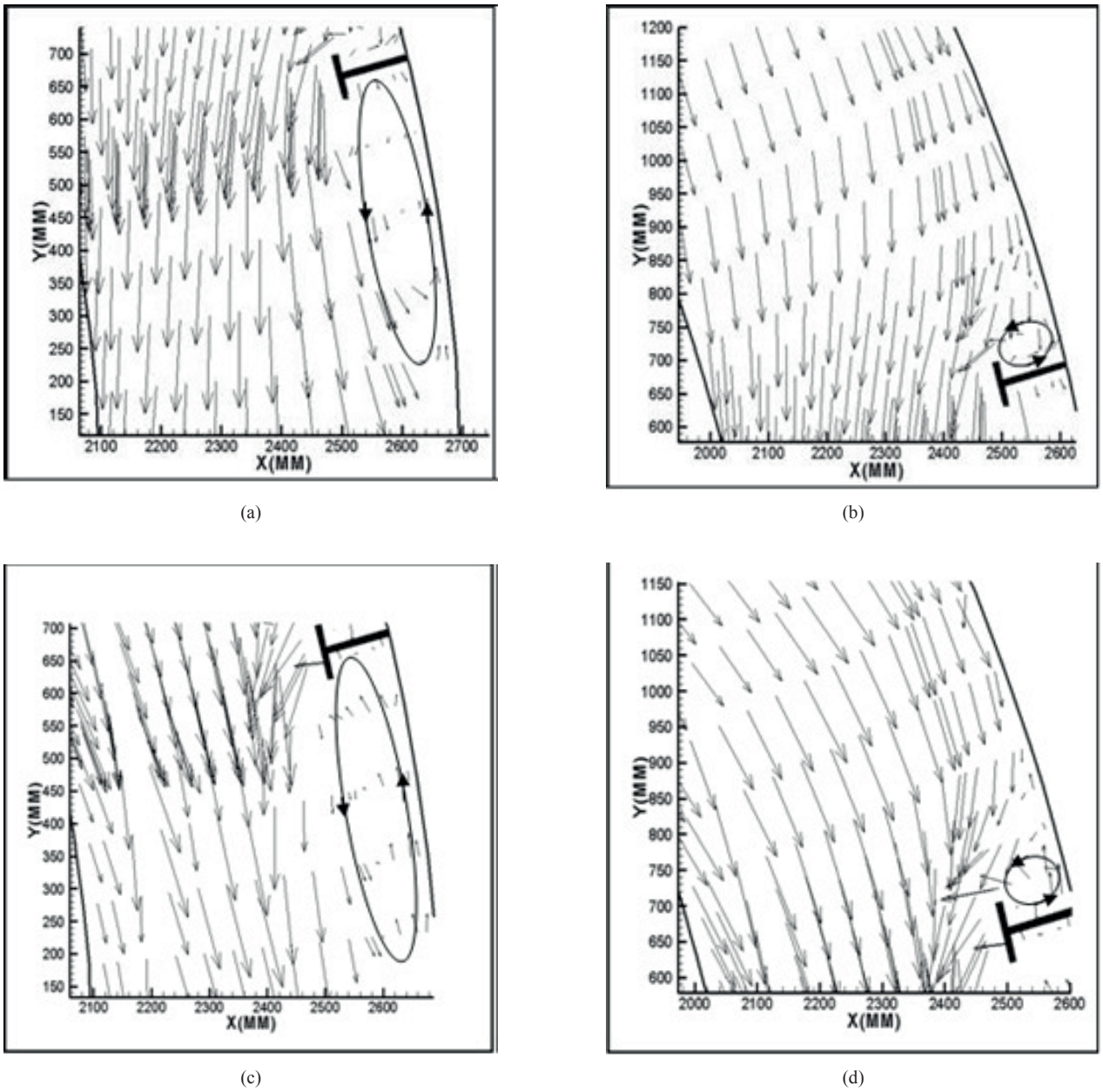

Fig. 10 Velocity vectors at distances of: (a) 5 mm from bed in the downstream; (b) 5 mm from bed in the upstream; (c) 115 mm from bed in the down stream and (d) 115 mm from bed in the upstream

depicted in Fig. 10(a). A strong vortex with counterclockwise direction is visible at the downstream of spur dike and close to the outer bank of channel. At the upstream of the spur dike, a horizontal vortex having dimensions equal to the spur dike length with counterclockwise direction is clear as shown in Fig. 10(b). The overall direction of vectors provides evidence that the spur dike is influential in diverting the flow towards the inner bank. The velocity vectors near the water surface at the downstream of the spur dike are shown in Fig. 10(c). A counterclockwise vortex of about 5 times the spur dike length and as wide as the spur dike length is formed in the upstream of the spur dike near the outer bank. The low-pressure zone at the downstream of the spur dike (near the outer bank) is the cause of formation of this vortex. Fig. 10(d) shows flow vectors in the upstream of the spur dike and near the surface. Another vortex of the same dimensions and the same direction as that in Fig. 10(b) is observable in this case. The comparison between vectors in Figs.10(a) and 10(b) and those in Figs. 10(c) and 10(d) makes it clear that the spur dike is more effective in diverting the near bed velocity vectors towards the inner bank than in diverting surface velocity vectors.

There are two major criteria for studying the secondary flows in channels with bend which are discussed here. Shukry in 1949, studied the flow along the bend and described secondary flow mechanism. He also presented following criterion for measuring the strength of secondary flow [19]:

$$S_{xy} = \frac{K_{lateral}}{K_{main}} \tag{1}$$

Where; S_{xy}: Strength of secondary flow; $K_{lateral}$: kinetic energy of lateral flow and K_{main}: kinetic energy of main flow.

For channels with bend, strength of secondary flow reflects that the tendency of flows to move towards the outer bank. Using Eq. (2), secondary flow strength is defined as [21]:

$$S_{xy} = \frac{\left(\frac{V_{xy}^2}{2g}\right)}{\frac{V^2}{2g}} \quad (2)$$

Where:

$$V_{xy} = \left(v^2 + w^2\right)^{0.5} \quad (3)$$

$$V = \left(u^2 + v^2 + w^2 + \right)^{0.5} \quad (4)$$

In Eqs. (3) and (4), *u*, *v*, and, *w* are longitudinal, lateral and vertical components of velocity through the channel, respectively, and g is the acceleration of gravity.

There is another criterion which helps to describe the influence of secondary flow in a channel bend named as vorticity. For an element with the dimensions $\Delta x * \Delta Y$ (see Fig. 11), the net rate of counter clockwise rotation of element about the normal axis is defined as follows:

$$\omega_z = \frac{1}{2}\left(\frac{\partial u}{\partial y} - \frac{\partial v}{\partial x}\right) \quad (5)$$

Where; ω_z: vorticity about the z axis; u: lateral component of velocity; and v: vertical component of velocity.

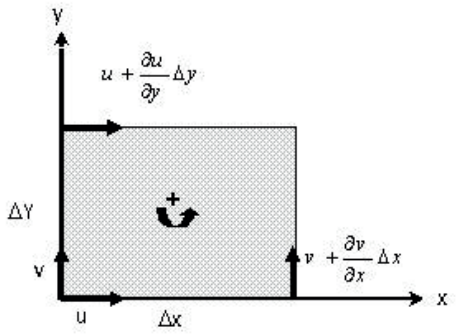

Fig. 11 Schematic diagram of element circulation

Fig. 12 shows the variations of secondary flow and vorticity along the bend with spur dike at section 75° as computed by using Eqs. (1) and (5). It is obvious that results of both methods follow the same trend along the bend. The maximum value occurs at about section 74°. This section is on the edge of the spur dike wing and the deepest scouring can be expected to form at this section, in case of movable bed. Between sections 74° and 82.5°, the values of both the parameters decrease. Thereafter, the values of these parameters increase with a small rate up end of the bend.

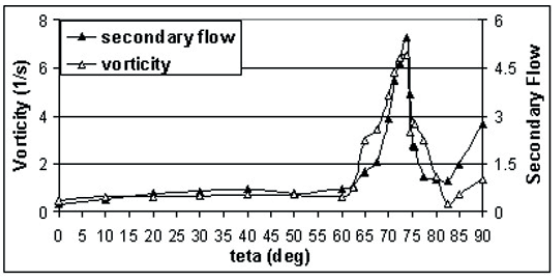

Fig. 12 Schematic diagram of element circulation

4 Conclusions

The flow field around a T-shaped spur dike with rigid bed was investigated in this study. The main results of this experimental study are:

1. In section 30° of the bend, secondary flow is formed near the inner bank and in the upper layers of the flow. The secondary flow continues to exist up to section 65° while wavering and becoming weak.
2. Lateral components of velocity profiles at section 72.5°, i.e. at an upstream distance of 1.2 times the length of spur dike, indicates the formation of two secondary flows. A counter clockwise flow is formed near the bed and another counter clockwise l flow forms near the water surface. Within the other 3/4 of channel width (between the vicinity of spur dike and inner bank) two other lateral flows are observed.
3. At lower section at a distance of 0.65 times spur dike length two lateral flows near the outer bank collapse into one lateral flow. At another section, near the spur dike web, at a distance of 0.25 times spur dike length, there are two lateral flows between the spur dike web and the outer bank. The first flow, which exists near the bed, is in the clockwise direction and the second lateral is in the counter clockwise direction. Between wing wall and the inner bank, the clockwise main secondary flow and a counter clockwise lateral flow, is observed.
4. A main secondary flow and second lateral flow forms at the downstream of the spur dike wing. A lateral flow also forms at the upstream of the spur dike wing.
5. In the section near the spur dike web, at a distance of 0.25 times the spur dike length, between the spur dike wing and outer bank, a counter clockwise weak lateral flow forms near the water surface.
6. Longitudinal component of velocity increases at first and second layers near the bed and near the wing of spur dike.
7. In sections close to the spur dike wing, longitudinal components of velocities at first and second layers near the wing are higher. By moving to the downstream direction of the bend, longitudinal components of velocities at the upper and middle layers grow. Near the outer bank of bend, the magnitude of velocity is less.

8. In the upstream of the spur dike, a horizontal counter clockwise vortex, with the dimensions equal to the spur dike length is formed. A counter clockwise vortex 5 times the spur dike length and as wide as the spur dike length is formed in the downstream of the spur dike near the outer bank.
9. The variations of strength of secondary flow and vorticity follow the same trend along the bend. They reach their maximum value at section 74° of the bend. Between sections 74° and 82.5°, both these parameters decrease. Thereafter, the values of these parameters increase with a small rate up to end of the bend.

References

[1] Giri, S., Shimizu, Y., Surajate, B. "Laboratory measurement and numerical simulation of flow and turbulence in a meandering-like flume with spurs." *Flow Measurement and Instrumentation*. 15(5), pp. 301-309. 2004. https://doi.org/10.1016/j.flowmeasinst.2004.05.002

[2] Nagata, N., Hosoda, T., Nakato, T., Muramoto, Y. "Three-dimensional numerical model for flow and bed deformation around river hydraulic structures." *Journal of Hydraulic Engineering*. 131(12), pp. 1074-1087. 2005. https://doi.org/10.1061/(ASCE)0733-9429(2005)131:12(1074)

[3] Fazli, M., Ghodsian, M., Salehi Neyshabouri, S. A. A. "Scour and flow field around a spur dike in a 90 bend." *International Journal of Sediment Research*. 23(1), pp. 56-68. 2008. https://doi.org/10.1016/S1001-6279(08)60005-0

[4] Ghodsian M, Vaghefi, M. "Experimental study on scour and flow field in a scour hole around a T-shaped spur dike in a 90° bend." *International Journal of Sediment Research*. 24(2), pp. 145-158. 2009. https://doi.org/10.1016/S1001-6279(09)60022-6

[5] Zhang, H., Nakagawa, H., Kawaike, K., Baba, Y. "Experiment and simulation of turbulent flow in local scour around a spur dyke." *International Journal of Sediment Research*. 24(1), pp. 33-45. 2009. https://doi.org/10.1016/S1001-6279(09)60014-7

[6] Duan, J.G., He, L., Fu, X., Wang, Q. "Mean flow and turbulence around experimental spur dike." *Advances in Water Resources*. 32(12), pp. 1717-1725. 2009. https://doi.org/10.1016/j.advwatres.2009.09.004

[7] Naji Abhari, M., Ghodsian, M., Vaghefi, M., Panahpur, N. "Experimental and numerical simulation of flow in a 90˚ bend." *Flow Measurement and Instrumentation*. 21(3), pp. 292-298. 2010. https://doi.org/10.1016/j.flowmeasinst.2010.03.002

[8] Duan, J.G., He, L., Fu, X., Wang, Q. "Turbulent burst around experimental spur dike." *International Journal of Sediment Research*. 26(4), pp. 471-476. 2011. https://doi.org/10.1016/S1001-6279(12)60006-7

[9] Gu, Z. P., Akahori, R., Ikeda, S. "Study on the transport of suspended sediment in an open channel flow with permeable spur dikes." *International Journal of Sediment Research*. 26(1), pp. 96-111. 2011. https://doi.org/10.1016/S1001-6279(11)60079-6

[10] Chen, L. P., Jiang, J. C., Deng, G. F., Wu, H. F. "Three-dimensional modeling of pollutants transportation in the flow field around a spur dyke." *International Journal of Sediment Research*. 27(4), pp. 510-520. 2012. https://doi.org/10.1016/S1001-6279(13)60009-8

[11] Sharma, K., Mohapatra, P. K. "Separation Zone in Flow past a Spur Dyke on Rigid Bed Meandering Channel." *Journal of Hydraulic Engineering*. 138(10), pp. 897-901. 2012. https://doi.org/10.1061/(ASCE)HY.1943-7900.0000586

[12] Vaghefi, M., Ghodsian, M., Salehi Neyshabouri, S. A. A. "Experimental study on the effect of a T-Shaped spur dike length on scour in a 90 degree channel bend." *Arabian Journal for Science and Engineering*. 34(2B), pp. 337-348. 2009. http://ajse.kfupm.edu.sa/articles/342B_P.06.pdf

[13] Vaghefi, M., Ghodsian, M., Salehi Neyshabouri, S. A. A. "Experimental study on scour around a T-Shaped spur dike in a channel bend." *Journal of Hydraulic Engineering*. 138(5), pp. 471-474. 2012. https://doi.org/10.1061/(ASCE)HY.1943-7900.0000536

[14] Vaghefi, M., Ghodsian, M., Adib, A. "Experimental study on the effect of Froude Number on temporal variation of scour around a T-shaped spur dike in a 90 degree bend." *Applied Mechanics and Materials*. 147, pp. 75-79. 2012. https://doi.org/10.4028/www.scientific.net/AMM.147.75

[15] Karami, H., Basser, H., Ardeshir, A., Hosseini, S. H. "Verification of numerical study of scour around spur dikes using experimental data." *Water and Environment Journal*. 28(1), pp. 124-134. 2014. https://doi.org/10.1111/wej.12019

[16] Fang, H., Bai, J., He, G., Zhao, H. "Calculations of Nonsubmerged Groin Flow in a Shallow Open Channel by Large-Eddy Simulation." *Journal of Engineering Mechanics*. 140(5), pp. 4001-4016. 2013. https://doi.org/10.1061/(ASCE)EM.1943-7889.0000711

[17] Ibrahim, M. M. "Local bed morphological changes due to oriented groins in straight channels." *Ain Shams Engineering Journal*. 5(2), pp. 333-341. 2014. https://doi.org/10.1016/j.asej.2013.12.006

[18] Vaghefi, M., Ahmadi, A., Faraji, B. "The Effect of Support Structure on Flow Patterns Around T-Shape Spur Dike in 90° Bend Channel." *Arabian Journal for Science and Engineering*. 40(5), pp. 1-9. 2015. https://doi.org/10.1007/s13369-015-1604-2

[19] Vaghefi, M., Ghodsian, M., Salehi Neyshabouri, S. A. A. "Experimental study on 3-D flow and scour pattern in a 90 degree bend." *Journal of Hydraulic*. 3(3), pp. 41-57. 2008. (in Persian).

[20] Shukry, A. "Flow around bends in an open flume." *Transactions of the American Society of Civil Engineers*. 115, pp. 751-779. 1950. http://cedb.asce.org/cgi/WWWdisplay.cgi?292033

[21] Vaghefi, M., Akbari, M., Fiouz, A. R. "An Experimental study of mean and turbulent flow in a 180 degree sharp open channel bend: secondary flow and bed shear stress." *KSCE Journal of Civil Engineering*, pp. 1-12.